

А. Иванисик, канд. физ.-мат. наук, П. Коротков, д-р физ.-мат. наук, Киевский национальный университет имени Тараса Шевченко, радиофизический факультет, кафедра медицинской радиопизики
Г. Понежа, канд. физ.-мат. наук, Национальная академия статистики, учета и аудита, Экономико-статистический факультет

СУБНАНОСЕКУНДНЫЕ ИМПУЛЬСЫ ВЫНУЖДЕННОГО КОМБИНАЦИОННОГО РАССЕИВАНИЯ ЛАЗЕРА С МОДУЛЯЦИЕЙ ДОБРОТНОСТИ РЕЗОНАТОРА ПРИ САМОФОКУСИРОВАНИИ

Результаты экспериментальных исследований подтверждают перспективность использования самофокусирующих сред для создания высоко эффективных преобразователей лазерного излучения на основе вынужденного комбинационного рассеивания. Показано, что благодаря динамике самофокусирования, в таких преобразователях можно изменить частоту и с использованием простой схемы компрессировать, более чем в десять раз, гигантские импульсы многомодовых лазеров. Предложенная и использованная схема применима для генерации инициирующих субнаносекундных стоксовых импульсов, которые далее могут использоваться для компрессии гигантских лазерных импульсов с соответствующим возрастанием мощности.

Ключевые слова: лазер, самофокусировка, вынужденное комбинационное рассеивание.

UDC 53; 547.136.13; 576.535; 577.037

O. Ivanyuta, Ph.D.
Department Electrophysics, Faculty of Radiophysics,
Taras Shevchenko National University of Kyiv

CHARACTERIZATION OF FULLERITY DERIVATIVES FOR ORGANIC PHOTOVOLTAICS

The fullerity C_{mn} derivatives were prepared by light illumination and ozonolysis of C_{60} gel solution. Experimental investigation was carried by UV-vis, IR, Raman spectroscopy, XPS and AFM. The structure of C_{mn} derivatives in gel solution (aggregates with hydrated shell) was studied. I present results from initial screening of the candidates based on informatics quantitative structure – property relationships, their comparison with results from density functional theory calculations about the effect of donor-acceptor architectures on the efficiency of the photovoltaic device. The comparison of spectral features for C_{mn} derivatives with the data for the adsorbed layers allowed to detect a series of C_{mn} hydroxyl group of derivatives.

Keywords: fullerity fullerol, hydroxyl-, epoxy-, keto- derivatives, electronic structure, surface-enhanced infrared absorption.

Introduction. Organic photovoltaic devices appear considerably cheaper and simpler in application, than traditional elements. Distribution of this technology is restrained by two important factors: not high (less than 9 %) efficiency of transformation and small works. It is considered that their commercial prospects depend on that, whether they will manage to attain ten percent efficiency at the simultaneous increase of calculation resource to ten thousand clock. These devices have recently reached 15 % efficiency and lifetimes close to 20 years; the search for the best (co)monomers for donor polymers being based on exacting experimental synthesis (Fig. 1).

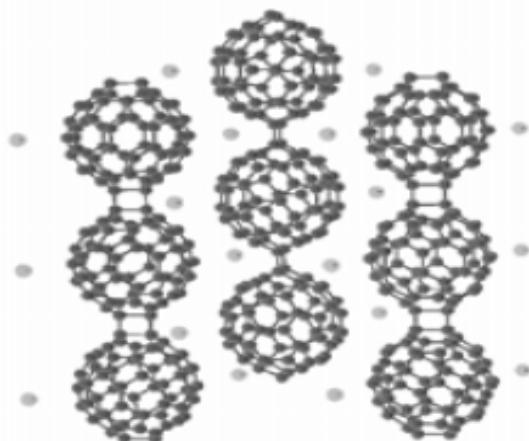


Fig. 1. Fullerity C_{m60} in polymer chains [1]

The design, automation and calculation of million organic molecules allow the screening of the best candidates for further study. Current applications of biosolutions with fullerity C_{m60} and they derivatives in molecular electronics are based on their behavior as active photosensitizer [1+5]. These features originate from known energy levels diagram (Fig. 2) of the photosensitized generation of singlet and triplet. Fullerity C_{m60} and its derivatives can be photosensitizer due to a strong absorption of light throughout the UV and visible regions and the low energy

gap between the excited singlet and triplet states (5,8 kcal/mol) facilitating efficient intersystem crossing. High yield of the triplet state, > 95%, provides an efficient generation of singlet excite. Also, C_{60} is a acceptor of photoelectrons with the ability to accommodate up to several electrons reversibly [1, 6].

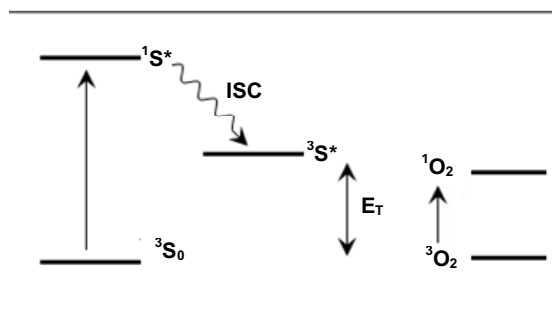


Fig. 2. Diagram of the energy levels in the photosensitized generation of singlet (1O_2). 1S , $^1S^*$, $^3S^*$ are the singlet ground state, the singlet excited state, and the triplet excited state, respectively, of the sensitizer S (C_{60}). 3O_2 and 1O_2 are the triplet ground and singlet state, respectively, of oxygen. Next transitions correspond: $^1S \rightarrow ^1S^*$ absorption; $^1S^* \rightarrow ^3S^*$ intersystem crossing (ISC); $^3S^* + ^3O_2 \rightarrow ^3S + ^1O_2$ energy transfer. The energy transfer is possible if $\Delta E_T > 100\text{kJ/mol}$ [1]

Physical and chemical properties of fullerity C_{m60} and they derivatives in gel solutions such as their structure (aggregates with hydrated shell), chemical and electronic structure were studied recently in respect to the photoinduced change transfer [1+5]. However, experimental investigation of the behavior of fullerity C_{m60} showed that it can be easily modification over light and very short time of charge transfer from donor to acceptor occurs [5, 8]. Also, the singlet excited exits very short time and these systems do not have applications in molecular electronic. Polymeric derivatives of fullerenes in solutions

also are of importance as photosensitizers, however their use in dissolutions needs special confirmations [3, 11].

In this work, synthesized gel soluble with fullerity C_{m60} derivatives by UV light illumination and ozonolysis of fullerene C_{60} gel solution. I consider also novel experimental data verifying hypothesis about possibility to prepare stable fullerity C_{m60} derivatives in gel solutions on C_{60} colloids. The comparison with the results of recent publication on fullerity C_{m60} [8÷12] was carried out. I present spectroscopic evidence of formation hydroxyl-, epoxy- and keto- derivatives and discuss variation of electronic structure of C_{m60} molecule associated with additions of the -O and -HO containing functional groups.

Experimental. I will show how the modification the electronic properties of the transparent electrode can be used to change the geometry of organic photovoltaic devices and build solar cells that do not require the use of low-work function electrodes. At the receipt of organic films the method Lengmyur - Blodzhett (a method allows to put

in order and orient molecules in monolayer by the set appearance) arises up problem of their thermal instability and distributions, appearing at the transfer of tape on samples [13, 21]. In addition, thickness of such tapes and, consequently, the stake of eaten up light is small. It does difficult the receipt of functional photo-electric devices on such organic tapes. Organic elements with more high efficiency of transformation (to 11 %) it is possible to get using the method of self organizations molecules, but from complication of this method the industrial production these devices is eliminated [19]. In order to study formation of gel solutions with C_{m60} hydroxyl-, epoxy- and keto-derivatives I prepared two types of C_{m60} gel solutions which from toluene C_{m60} solution followed by evaporation of the toluene overlayer spread on the strong and polymer surface [13, 15]: this C_{m60} gel solution was illuminated by UV light from a standard bacterium dead lamp in air, $T = 300$ K, 1 h. The tin layer gel solution was ozonolysis during 30 min, the toluene layer was evaporated on the strong and polymer surface, assisting the transfer of C_{m60} derivatives from toluene solution [3, 14]. Also, I studied C_{m60} derivatives in two toluene solutions: (1) products formed after ozonolysis C_{60} toluene solution were repetition dissolved in toluene (a saturated solution was produced); (2) the toluene solution (1) was illuminated by UV light in air by eximer laser 280 nm, $T = 300$ K, 1 h.

Absorption spectra of these products in gel and toluene solutions were recorded with double beam spectrometers Jasco V-570 or UV-2401PC in quartz cavettos with the range 190 ÷ 2500 nm at $T = 300$ K. Raman spectra of these products in toluene solutions in quartz glass cavettos were recorded by double monochromator DFS-24 or CT-25C with 514,5 nm excitation light of an Ar laser in range of the wave numbers 11200 ÷ 1500 cm^{-1} at $T = 300$ K.

Two types of C_{m60} derivatives in gel solutions were used for the fabrication of adsorbed layers on fianit and Al_2O_3 (100) substrates. Typically, 0,2·ml a solutions was dropped on a cleaned surface of TIBr (36 %)-TIJ (64 %) monocrystals and a specially treated surface Al_2O_3 (100) wafers (procedure used in [13]), and samples were dried in air at $T = 300$ K in dark. The samples with adsorbed layers

were studied with IR spectroscopy (fianit substrate) and XPS (Al_2O_3 (100) substrate). The SPECORD 75 IR Zeiss spectrometer for transmission spectra measurements in the range wave numbers 250 ÷ 4000 cm^{-1} and the combined spectrometer including XPS equipment with UV radiation ($h\nu = 1355$ ·eV) were used. Morphology of the adsorbed layers was studied with atomic force microscopy (AFM) at ambient conditions in the tapping mode [7, 10].

Results and discussion. Fullerity does not differ in high chemical activity [9]. To the moment of beginning studies in the world were not undertaken a systematic works on research of possibility forming fullerity C_{m60} the uncovalently constrained complexes, their physical properties were not studied. A few works were sanctified to the study of cooperation molecules in solutions [16, 18]. Fullerity possess photoconductivity in a spectral range optimal for creation of solar elements.

Basic efforts were concentrated on the study of the covalently-constrained systems of artificial photosynthesis. There were not works on the receipt of such structures in a thin film variant. An organic semiconductor donor-acceptor complex C_{m60} is perspective material for the receipt of molecular by volume heterostructures, thin films heterotransitions and creation of photovoltaic devices. In such solar cells both electrodes are comprised of conducting polymers that are modified to become either hole or electron collecting electrodes. Quantum-chemical calculations showed that complex C_{m60} formed the uncovalently constrained molecular complex, energy of connection that grows and equilibrium distance diminishes among Mg, Zn. The complete charge components complexes is expected. In particular, the realization of surface-enhanced infrared absorption (SEIRA) permitted one to speak of a unified field of surface-enhanced vibrational spectroscopy (SEVS), supported by the enhanced Raman and infrared techniques. Enhancement by SEIRA depends on the size, shape, and particle density of the selected metal island films. In the most widely used Al_2O_3 (100) configuration, film morphology is influenced by surface structure of the supporting substrate, as well as by the experimental conditions used during the film fabrication. An exact count gives the value of transfer charge of C_{m60} - TPP 0,002 elementary charge, in the complexes of C_{m60} - MgTPP and C_{m60} - ZnTPP – 0,2 and 0,4 elementary charge, accordingly.

The materials of the first group allow for transmission and/or reflection spectra, while the others are only adequate for external reflection measurements. Notably, low reflective materials could be optically favorable due to a reduced distortion of the band shape in the corresponding SEIRA spectrum. The spectrum photoabsorption C_{m60} lies in the length range waves 280 ÷ 680 nm and a quantum exit, being probability formation of electron - ionic pair at absorption one photon, 0,9 makes (Fig. 3). The absorption bands with maxima at 527, 573, 1088, 1183, 1220 and 1425 cm^{-1} were revealed in IR spectra of the C_{m60} derivatives layer formed by UV light illumination in air (Fig. 3, b). The maxima at 527, 573, 1183 and 1425 cm^{-1} correspond to the vibration modes of C_{m60} molecules [4, 16]. The bands are broad testifying that some derivatives can appear in water solution as the result of photooxidation [9], e.g. of $C_{60}O$ (epoxide) and $C_{60}(-OH)_k$ (fullerol).

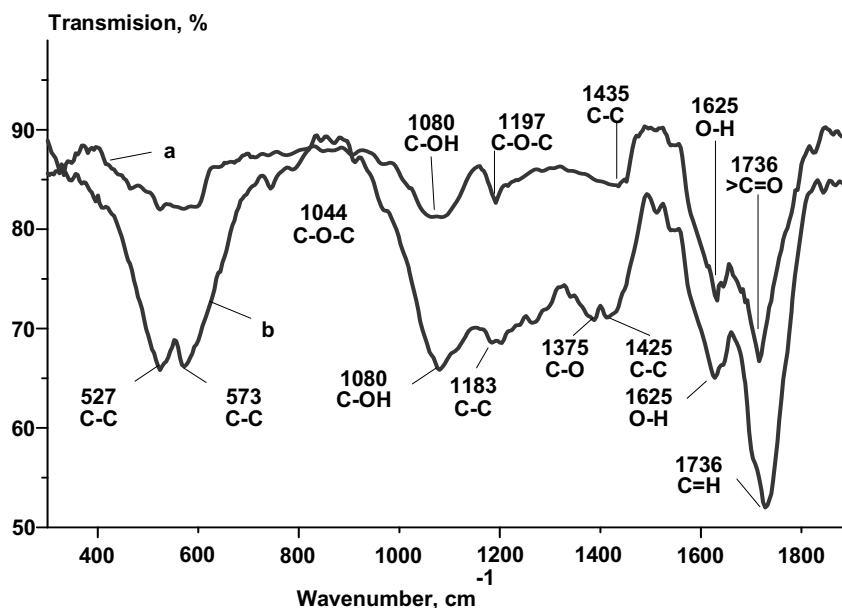


Fig. 3. SEIRA transmittance spectra of C_{m60} derivatives in adsorbed layers on Al_2O_3 (100) substrate from fullerene C_{60} derivatives formed by the different methods: a – ozonolysis; b – UV light illumination in air. The positions of the absorption bands for vibrational modes corresponded to $>C-O$, $>C=O$, $C-O-C$, $C-OH$, $-OH$ groups [3, 17] and to vibrational modes of C_{60} molecules in gel solution [22] are marked. The insert is the spectrum (a) in the range $300 \div 1900 \text{ cm}^{-1}$

Polymerization fullerene C_{60} under the action of light radiation and formation insoluble in organic solvents tape allow using fullerene as new material for photo resistance cells. The band at 1080 cm^{-1} may be attributed to vibrations of $C-OH$ bonds. The vibration mode of $C-O$ bonds in epoxides appearing at 1374 cm^{-1} was revealed also. The vibration mode at 1376 cm^{-1} is attributed to vibrations of $>C-O$ bonds in epoxides, at 1197 cm^{-1} does vibrations of $C-O-C$ ester groups, and the intensive band at 1736 cm^{-1} looks as contribution due to ketone group $>C=O$ [7, 18]. A prolonged illumination of this layer during 4 h at air (relative humidity 70 %) caused destruction of the part of $C-OH$ bonds in $C_{60}(-OH)_k$ since in the IR spectrum the intensity of 1380 cm^{-1} vibration mode strongly decreased. This result confirms that part of $C_{60}(-OH)_k$ bounds can be destroyed. In IR spectra of the layer produced by ozonolysis absorption bands with maxima at 1197, 1375, 1646, 1736, 3226 and 3421 cm^{-1} occurred (Fig. 4). The bands at 1620 and 3306 cm^{-1} can be attributed to deformation and stretching vibrations of adsorbed $-OH$ groups, correspondingly. The other vibration mode of $C-OH$ also makes the contribution in range $3290 \div 3300 \text{ cm}^{-1}$.

This was confirmed also by comparison of the Raman spectrum C_{m60} derivatives formed by ozonolysis and redissolved and formed in gel by UV light illumination in air at $T = 300 \text{ K}$. I revealed that in the first spectrum the peak at 1437 cm^{-1} and in the second spectrum the peaks at 1443 and 1461 cm^{-1} appear. Assuming that the peak at 1437 cm^{-1} corresponds to the peak at 1443 cm^{-1} in the second spectrum, the position of the peaks in the first and the second spectrums can be due to ketone and epoxides groups, respectively. This assumption based on the

comparison of the positions of the peak at 1461 and 1469 cm^{-1} which is known for solid C_{m60} and C_{60} molecule [4, 16]. The position of these peaks (at 1443 and 1461 cm^{-1}) can inform on different degree C_{60} oxidation in these two solutions. The next evidence of possible formation of C_{m60} derivatives tailed by $>C-OH$ and $>C=O$, $C-O-OH$, $C-O-C$ groups in the adsorbed layers was obtained from the data of XPS experiment for $C1s$ photoemission line (Fig. 5). The spectrum was deconvoluted through the least-squares procedure fitting raw spectra to Gaussians. For C_{m60} derivatives formed by ozonolysis the positions of Gaussian maxima are $h_b = 285,2 \cdot \text{eV}$, 285,6, and $h_b = 285,8 \cdot \text{eV}$. The reference binding energy of $C-C$ bonds in C_{60} is $285,2 \cdot \text{eV}$ [10, 19], and for $C-OH$ bonds the values $h_b = 286,5 \cdot \text{eV}$ and $h_b = 285,6 \cdot \text{eV}$ can be assigned to $C-O$ or $C=O$, respectively [11].

For the sample produced by UV light illumination in air the energy positions of Gaussians for the $C1s$ line are 285,2, 285,4, 286,8, $287,7 \cdot \text{eV}$ (Fig. 6). These maxima were assigned to $C-C$ bonds in C_{m60} ($h_b = 285,2 \cdot \text{eV}$), $C-OH$ bonds ($h_b = 285,4 \cdot \text{eV}$), in $C=O$ or $O-C-O$ bonds ($h_b = 285,6 \cdot \text{eV}$) and in $C-O-OH$ bonds ($h_b = 287,7 \cdot \text{eV}$) [10, 12]. The energy position Gaussian maximum at $h_b = 287,7 \cdot \text{eV}$ can correspond to the mono-oxygenated carbon in fullerol [12, 18]. These conclusions mainly confirmed by data for $O1s$ photoemission line those will be publish elsewhere. Thus, these results indicate on formation of $>C-OH$, $>C=OH$, $C-O-OH$, $>C=O$, $C-O-C$ bonds for fullerene C_{60} oxygen derivatives, and the skeleton of C_{m60} molecule, probably, is not broken.

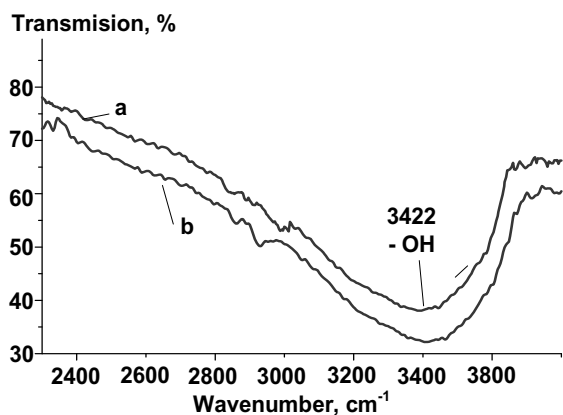


Fig. 4. SEIRA transmittance spectra of C_{60} derivatives in adsorbed layers on Al_2O_3 (100) substrate from C_{60} derivatives formed by the different methods: a – ozonolysis; b – UV light illumination in air.

The insert is the spectrum in range $2300 \div 3900 \text{ cm}^{-1}$.

The vibration mode at 3422 cm^{-1} was attributed to stretching vibrational mode of adsorbed -OH groups

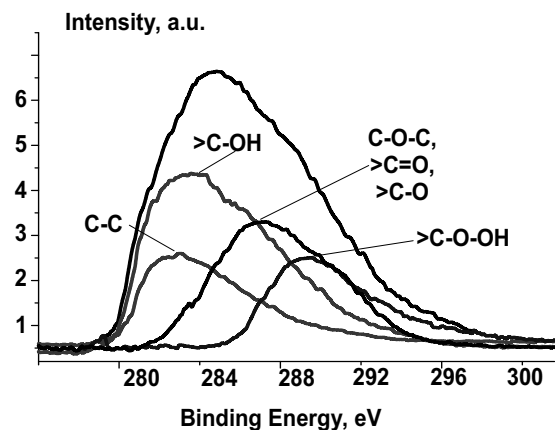


Fig. 5. C_{1s} XPS spectra C_{60} derivatives in adsorbed layers on Al_2O_3 (100) formed by the different methods ozonolysis in air. The positions of the peaks are centered at binding energy corresponded to >C-OH, C-C, C-O-C, >C=O, >C-O, C-O-OH bonds

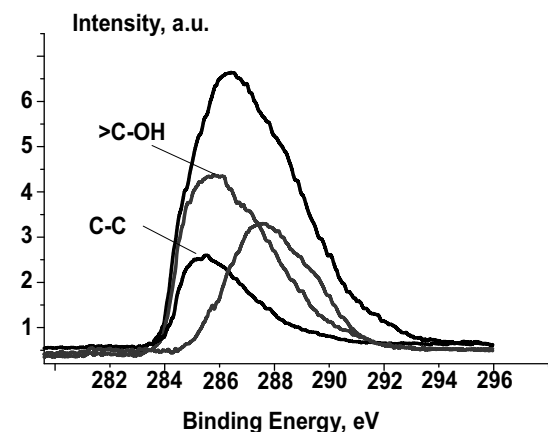


Fig. 6. C_{1s} XPS spectra of C_{60} derivatives in adsorbed layers on Al_2O_3 (100) formed by the different methods UV light illumination in air. The positions of the peaks are centered at binding energy corresponded to >C-OH, C-C bonds

Because, the value of binding energy for C-C bond ($h_b = 285,2 \cdot \text{eV}$) are near to the value respective the bonds on the skeleton C_{60} . Using the above analysis of absorption bands in IR and XPS data for C_{60} derivatives prepared by ozonolysis (Fig. 3, 4 and Fig. 6) corresponding to C_{60} molecule tailed by ketones (>C=O), esters groups (C-O-C), and hydroxyl (>C-OH) the percent ratio of these component was evaluated: >C=O – 34%, >C-OH – 22 % and C-O-C – 19,5 %. These C_{60} tailed molecules shown in Fig. 6.

The aggregates of C_{60} derivatives on substrates From our earlier AFM studies [3, 15] for C_{60} oxygen and hydroxyl group derivatives in adsorbed layer on dielectric substrates formed over UV light illumination in air established that this layer contains planar orientation aggregates with length up 135 \AA including the two C_{60} molecular clusters. Every cluster with 11 molecules of C_{60} (28 \AA) has the diameter up 72 \AA . Between these aggregates small aggregates appear with length up 50 \AA from two $(C_{60})_{11}$ molecular clusters with the diameter 25 \AA and/or crystallites C_{60} with linear size up $28,6 \text{ \AA}$. These cluster systems form one-dimensional chains due to self-organization over UV light illumination.

Several interesting nanoarrays C_{60} were also found in UHV environment. Hydrogen bond based network structures provide a potential pathway to the design of host-guest interfaces, because the cavity size can be controlled through careful selection of the component molecules. The formation of a self-assembled bimolecular network C_{60} through hydrogen bonds by co-adsorption of perylene tetracarboxylic di-imide (PTCDI) and 1, 3, 5-triazine – 2, 4, 6 triamine (melamine) was reported [11, 20]. AFM images obtained by within the framework of this work for adsorbed layer from C_{60} derivatives formed by ozonolysis show, in contrast to described morphology of the adsorbed layer with C_{60} derivatives formed over UV light illumination in air, disordered spherical particles with diameter $80 \div 120 \text{ nm}$ which can be evaluated as the clusters of C_{60} derivatives comprising $114 \div 171$ molecules C_{60} (7 \AA).

Electronic spectra of C_{60} derivatives to show in Fig. 7. On the basis of these result I propose the energy diagrams and electronic transitions in C_{60} [3, 14]. and their correlation with possible electronic structure of C_{60} molecules tailed by -O and -OH group. Three and two intense broad absorption bands with maxima at 220, 265, 345 nm and with minimum at 241, 284, 336 nm (Fig. 7, a) dominate in the range $190 \div 410 \text{ nm}$ for the spectra in gel and toluene solutions. The energy positions of these maxima correspond to allowed electron transitions $h_g, g_g \rightarrow t_{2u}$ (218 nm), $h_u \rightarrow h_{2g}$ (264, 284 nm) and $h_g, g_g \rightarrow t_{1u}$ (340, 336 nm) (Fig. 7). The shifts between the maxima in gel and toluene solutions are 20 and 40 nm. They can be associated with the hydration of C_{60} in gel solution influencing an occupation of lowest state conductive band, which created by molecular states t_{1u} . It is important also for electron transitions $h_g, g_g \rightarrow t_{1u}$ and / or their hydrated aggregates self-formation [4, 5]. The

revealed morphology of adsorbed layer from this solution on substrate confirms it. The lowest allowed electron transition $h_u \rightarrow t_{1g}$ to excited state T_{1u} at 408 nm is revealed only in spectra of the C_{m60} derivatives in toluene formed by ozonolysis. This electron transition is allowed only for solid C_{m60} (Fig. 8) [4, 21].

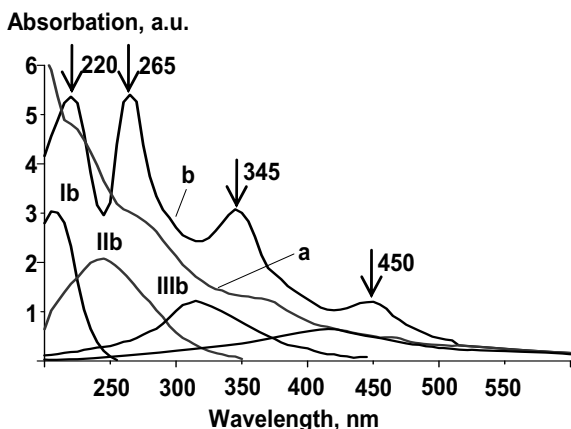


Fig. 7. The absorption spectra of solutions produced by the following procedures: a – UV light illumination of C_{m60} gel solution in air; b – ozonolysis of C_{m60} in toluene solution. Deconvolution of the spectrum (b) shows positions of four bands, residuals are scarcely evident. The positions of Ib, IIb, IIIb bands are at 203, 242, 312, 421 nm, respectively. The insert is these absorption spectra in the energy scale ($1,5 \div 2,5 \cdot eV$)

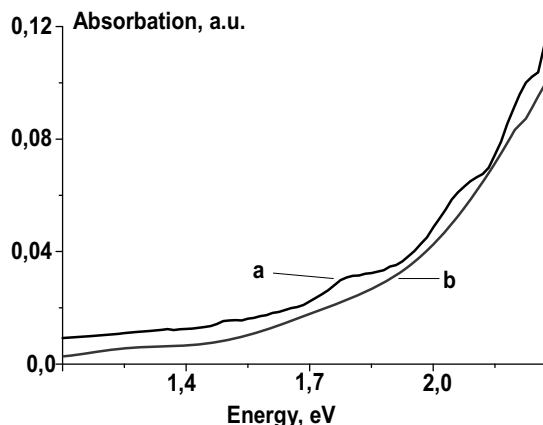


Fig. 8. The positions of the absorption edges in spectra (a) and (b) of C_{m60} derivatives in gel can be revealed at 1,7, 1,8 · eV , respectively

In the range $420 \div 640$ nm the bands can be associated with electronic transitions to the excited states. The spectra of C_{m60} derivatives in gel and in toluene show the weak bands near 450, 621 nm (Fig. 9, d) and 536, 598, 624 nm (Fig. 10, a), respectively. The weak band at 450 nm in spectrum in gel corresponds to minimum absorption near 440 nm in spectrum in toluene (curves d and a, respectively), and the known electronic transition $2,75 \cdot eV$ (450 nm) can be identified as $h_u \rightarrow t_{1g}$ transitions in solid C_{m60} for these maxima [5, 14]. Also, the weak bands near 620 nm (621 and 624 nm) occur in both spectra. It is known that in the range

$490 \div 640$ nm ($1,9 \div 2,5$ eV) the weak absorption takes place associated with electric dipole-forbidden transitions between the one-electron HOMO level with h_u symmetry and one-electron t_{1u} LUMO level. Only for the solution of C_{m60} derivatives in toluene the weak absorption at 536 and 598 nm are (Fig. 9, a) [3, 19]. I suppose that the spectrum in Fig. 6 can characterize the solid C_{m60} rather than free C_{m60} molecules. These absorption maxima are shifted (up to 10 nm) in comparison with known positions of the solid C_{m60} (460 and 625 nm, respectively).

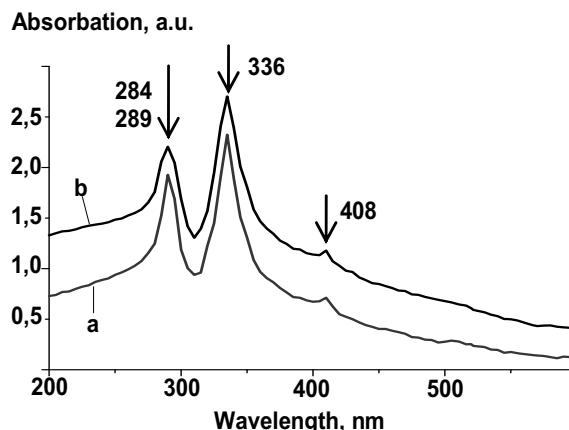


Fig. 9. Absorption spectra of C_{m60} (a) and C_{60} oxygen derivatives (b) in gel solution

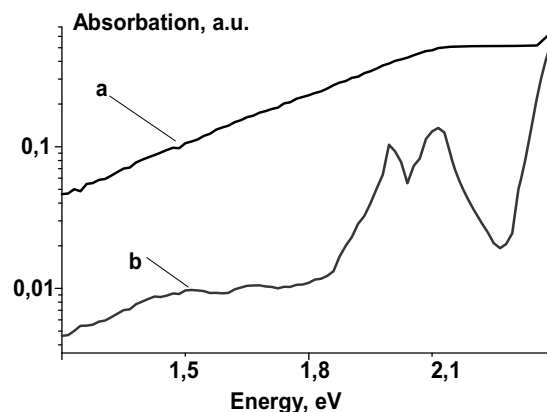


Fig. 10. The positions of the absorption edges for the spectra (a) and (b) can be evaluated at 1,95 and 2,11 · eV , respectively. The insert is these absorption spectra in the energy scale ($1 \div 3 \cdot eV$)

The difference between shapes of absorption spectra in the range $410 \div 550$ nm for C_{m60} derivatives in gel and toluene can be interpreted assuming that $C_{m60}O_n$ absents in toluene, the minimum at 440 nm occurs (Fig. 11, a). Hence, the higher absorption in this range for spectra prepared without (Fig. 11, d) and with ozonolysis of initial solution of C_{m60} derivatives in toluene (Fig. 11, c) confirm that $C_{m60}O_n$ can be in both solutions. In gel solution of C_{m60} derivatives prepared without ozonolysis of initial solution of C_{m60} in toluene the features due to $C_{m60}O_n$ are observed (that was showed in analysis of IR spectra in Fig. 3, a) [4, 12].

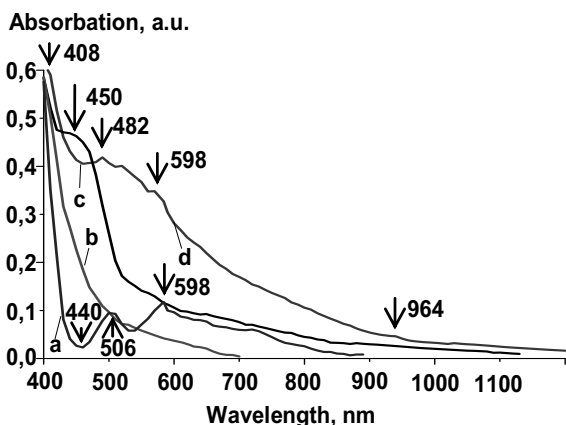


Fig. 11. The absorption spectra of C_{60} in toluene solution (a) and C_{60} derivatives in gel solutions prepared by UV light illumination of gel solution in air (d) and toluene solution (c), (b) corresponds to gel solution prepared from ozonolysed C_{60} toluene solution

In order to built energy diagram (Fig. 12) of the electronic transitions corresponding to the above experimental data we take the known calculated value for the HOMO–LUMO gap in C_{60} single molecule equal to ~ 1.5 eV [14, 22] and assume that the HOMO – LUMO electronic transition in hydrated C_{60} and $C_{60}O$ molecules and aggregates with ordered structure in water is 1.7 eV (insert in Fig. 8, a) and similar electron transitions in C_{60} molecules in toluene is at 1.8 eV (insert in Fig. 9, a). The comparison between electronic spectra of C_{60} derivatives in gel solution formed by ozonolysis (Fig. 7, b) and C_{60} oxygen derivatives in gel solution formed over UV light illumination

in air (Fig. 7 a) indicates the clear difference of the first with appearance of absorption bands Ib, IIb, IIIb. Positions of band centers 220, 265, 345 nm are shifted to lower wavelengths as compared with those corresponding to electric dipole-allowed electron transitions between HOMO and LUMO in C_{60} molecule (and also in their analogs in solid C_{60}).

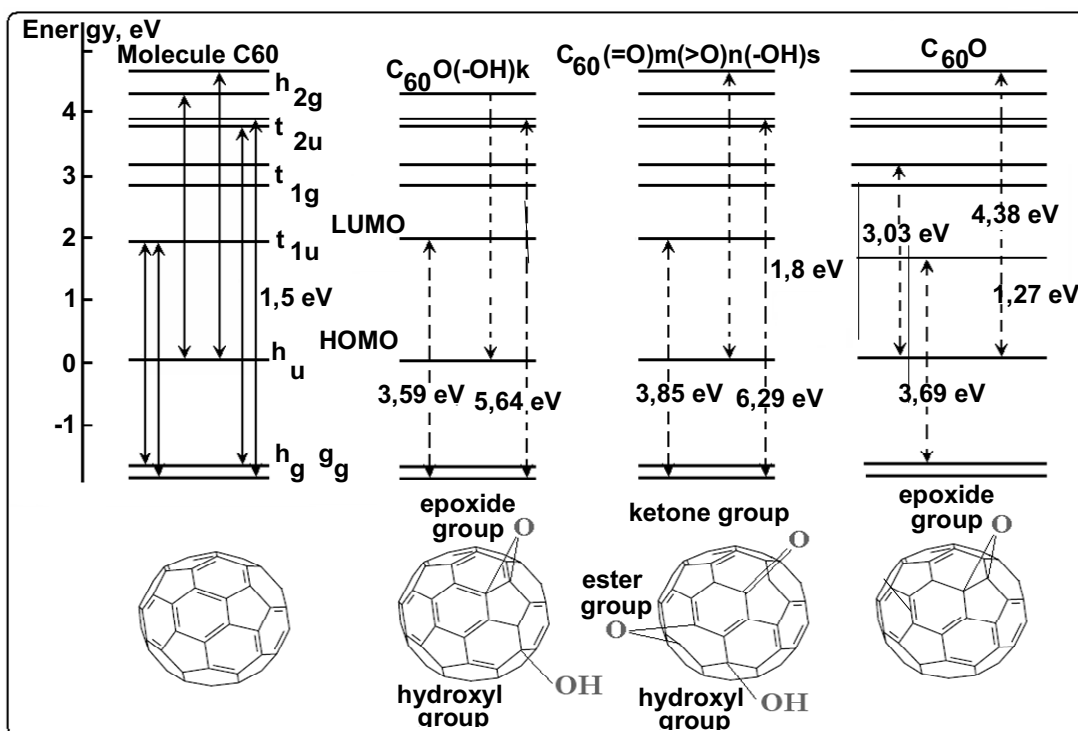


Fig. 12. IR transmittance spectra of C_{60} derivatives in adsorbed layers on Al_2O_3 (100) substrate from C_{60} derivatives formed by the different methods: a – ozonolysis; b – UV light illumination in air. The positions of the absorption bands for vibrational modes corresponded to $>C-OH$, $>C=OH$, $C-O-OH$, $>C=O$, $C-O-C$, $C-OH$, $-OH$ groups [7, 12] and to vibrational modes of C_{60} molecules are marked [3, 8]. The insert is the spectrum (a) in the range $2500 \div 4000 \cdot cm^{-1}$. The vibration mode at $3306 \cdot cm^{-1}$ was attributed to stretching vibrational mode of adsorbed $-OH$ groups

The photo – reactive monolayer was formed by the adsorbate molecule bearing a ketone group and a benzophenone moiety on an Au-deposited Al_2O_3 (100) substrate. UV exposure caused the benzo phenone moiety to induce the photochemical graft reaction with a thermoplastic hydrocarbon polymer. The photo-induced graft reaction suppressed the dewetting of a polymer thin film with a C_{60} on the Al_2O_3 (100) substrate. The dewetting suppression was achieved at an exposure dose of $5 J \cdot cm^{-2}$ at the irradiation wavelength of 254 nm. The dewetting

suppression enabled us to fabricate reliable fine patterns of the polymer film by thermal nanoimprint lithography and the Au film by subsequent wet etching. The positions of band Ib, IIb and IIIb are 197, 249 and 322 nm (6.29, 4.97 and $3.22 \cdot eV$). These results are confirmed for the spectra of the diluted solution in gel: it leads to decrease of the absorption throughout the whole range. The observed shifts of Ib, IIb, IIIb bands positions were interpreted as the formation of $C_{60}(=O)_m(>O)_n(-OH)_s$ taking into account the IR spectra in presented Fig. 3, a, and analysis of the

spectra of C_{m60} derivatives in gel solution, toluene (Fig. 5, 6, a). They are consistent also with variations of absorption features of C_{m60} molecule in after light irradiation and photolysis [11]. In Fig. 7 the electronic transitions with energy corresponding to the maxima Ib, IIb, IIIb for $C_{m60} (= O_m)(> O)_n(-OH)_s$ are presented. Self-assembled 2D structures of C_{m60} derivatives have been a prime target for observations by atomic force microscopy (AFM). I observed that molecules of C_{m60} form a 2D network on $Al_2O_3(100)$ substrate, driven by attractive intermolecular interactions [5, 17], while the surface migration barriers are comparatively small and charge transfer to the adsorbed molecules is minimal. On the contrary, a significant charge transfer is observed in repulsive forces between the molecules that prevent the formation of a molecular add layer network (see Fig.13). It was shown that the limiting factor in the formation of self-assembled networks C_{m60} is the nature of frontier orbital overlap and absorption interface electron transfer. Various patterns determined by the intricate interplay between directional hydrogen bonding interactions and packing forces, including chain molecule–molecule and C_{m60} substrate interactions, - demonstrated the possibility of programmed surface patterning using C_{m60} incorporating directional intermolecular interaction sites. I developed an effective and facile method for self-assembling C_{m60} molecules into hollow hexagonal nanoprisms with uniform size and shape and controllable aspect ratio [14, 16].

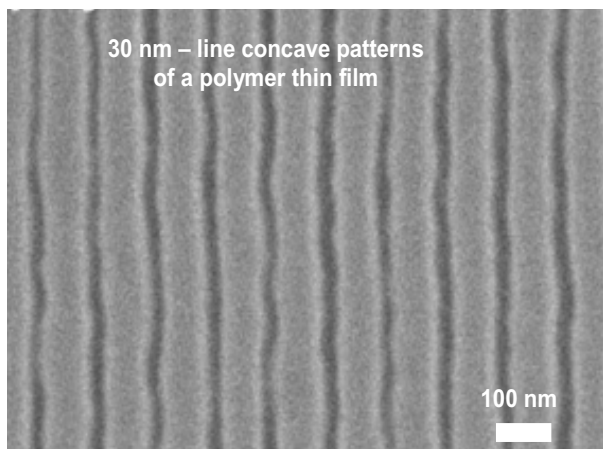


Fig. 13. The photo-induced graft reaction suppressed the dewetting C_{m60} of a polymer thin film on the $Al_2O_3(100)$ substrate. UV exposure caused the benzophenone moiety to induce the photochemical graft reaction with a thermoplastic C_{m60} polymer

The following features associated with $C_{m60} (= O_m)(> O)_n(-OH)_s$ compounds presence can be pointed out in the range 400 ÷ 1000 nm the spectra of C_{m60} derivatives in gel solution formed by ozonolysis in toluene and the spectra of C_{m60} derivatives in gel solution formed over UV light illumination in air (Fig. 11, a-d): the weak band at 408 nm corresponding to solid C_{m60} exists only in the absorption spectra of C_{m60} derivatives in toluene before and after ozonolysis (Fig. 11,a, c); the band near 450 nm with higher absorption as compared with curve a in the spectrum of C_{m60} derivatives in toluene after ozonolysis (Fig. 11, c);

the broad band at 482 nm in spectra of C_{m60} derivatives in toluene after ozonolysis (Fig. 11, c) which is remarkably shifted to shorter wavelengths compared to the band of C_{m60} derivatives in toluene after illumination (536 nm). These features of the oxidized and photolysed C_{m60} in solution were associated with $C_{m60}O$ formation [11, 15]. I can assume that HOMO-LUMO electronic transition with energies 1,9 and 1,27·eV (from insert in Fig. 10) can be due to C_{m60} molecular aggregates and $C_{m60}O$ in toluene, respectively. These electronic transitions for $C_{m60}O$ are presented in Fig. 12. In the spectral range 925 ÷ 1000·nm (Fig. 11) the weak feature can be assigned if to consider $C_{m60}O$ caption as a constituent of the excited $C_{m60}O$ compound, and analyze the vibration mode at 964·nm (1,34·eV). In the near - IR spectra this mode presents as the result of the electrochemical oxidation C_{m60} applying a potential sufficiently negative to cause the reduction of resulted in the regeneration of C_{m60} [6, 11].

I tested the functionality of the thermoplastic C_{m60} polymer and performed temperature - dependent conductivity measurements on the bulk powder materials.

It was the room temperature value for C_{m60} fell below the experimental limit. Therefore, no temperature dependence could be measured (Fig. 14). However, the modifying C_{m60} powder drastically increased by at least nine orders of magnitude compared to chains. Its temperature dependence resembled that of the C_{m60} , indicating that conduction occurred through a percolated three-dimensional network of C_{m60} . However, the room temperature value of the modifying C_{m60} composite did not reach the value of a C_{m60} network, which is expected to be one or two orders higher in magnitude. This indicates the existence of additional tunnelling barriers between the C_{m60} , formed by the coating around C_{m60} . As a further indication of functionality enhanced thermal stability of the composite, which decomposes in air higher. It investigated the photophysical properties of the composite and measured its photoluminescent behavior ($\lambda_{ext} = 330\cdot nm$). Shows, that's a broad emission maximum modifying C_{m60} at about 410·nm caused by reduced groups.

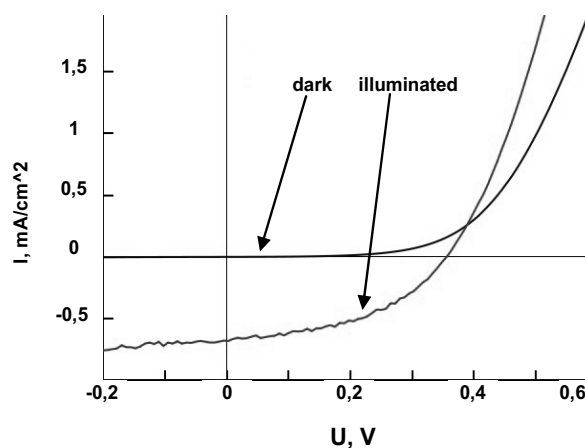


Fig. 14. I-V characteristics of inverted C_{m60} bulk-heterojunction solar cells with and without light modification

Another new concept for a solid-state cell consists of a polymer organic semiconductor that combines the functions of light-absorption and charge transport in C_{m60} material. Therefore, it's able to replace both the transporting excitation. The photoinduced charge separation at the interface of an organic semiconductor has been studied in relation to photovoltaic devices. For an efficient charge generation, it is important that the charge-separated state is the thermodynamically and kinetically most pathway after photoexcitation. Therefore, it's important that the energy of the absorbed photon is used for generation of the charge-separated state and is not lost via competitive processes like fluorescence 410 nm. In addition, it is of importance that the charge – separated state is stabilized, so that the photogenerated charges can migrate to two of the electrodes. Therefore, the back electron transfer should be slowed down as much as possible. When a polymeric semiconductor is excited across the optical band gap C_{m60} . The excitation energies and valence band was offsets of C_{m60} this molecular semiconductor may allow electron transfer to the conduction band of an inorganic semiconductor. It's excitation energies C_{m60} are no longer created at the interface only, but throughout the whole organic material for electronic devices.

Soluble modifying C_{m60} composite has enhanced conductivity and improved thermal stability. It's also luminescent, optically active and can be processed from solutions into films, coatings and fibres. Depending on the synthesis conditions, the bithiazole based polymers exhibited optical band gaps range $1,77 \div 2,62 \cdot eV$ and the copolymers displayed chromism within a wide span of the visible spectrum. These observations are consistent with the polymer adopting conformation. The circular dichromatic spectrum for modifying C_{m60} showed that the polymerization of aniline in the presence of C_{m60} and doping did not inhibit the polymer's ability to become optically active.

Conclusions. Finally, I will describe examples of organic solar cell architectures in which all layers are comprised of polymers that can be processed from solution. I believe that these strategies pave the way to very low-cost photovoltaic technologies with light-weight and flexible form factors. I present the spectroscopic study evidencing formation of hydroxyl-, epoxy- and keto-derivatives of C_{m60} and analyze changes in the electronic structure of C_{m60} molecule associated with additions of these functional groups. The skeleton of C_{m60} molecule is assumed not broken on the basis of IR, Raman, UV-Vis, XPS spectra of the C_{m60} derivatives. The electronic

transitions in the spectra of identified $C_{m60}O$, $C_{m60}O(OH)_k$ and $C_{m60}(=O)_n(>O)_n(-OH)_s$ are presented (see Fig. 12). These transitions can play a role in process of new photosensitizers. The copolymers revealed short switching times and useful optical contrast respectively. These devices exhibited low switching voltages and switching times with reasonable stability under atmospheric conditions. I believe that these findings provide the basis for novel smart organic materials of great use in smart optoelectronic applications and devices.

Reference

1. Cancer and aging as consequences of un-repaired DNA damage. In: New Research on DNA Damage / Ed. by Honoka Kimura, Aoi Suzuki. – New York., 2008.
2. Gorchinskyi, A.; Bukalo, V.; Scharff, P. et al. Self-Formation of Nanostructures from Hydrated Aggregates and Nanocrystals of $(C_{60})_n$ Molecules on the Liquid Crystal Layer. // In Book: Electronic properties of novel materials – science and technology of molecular nanostructures, New York. – 1999.
3. Frontiers of nano-optoelectronic systems / Ed. by L. Pavesi, E. Busaneva. – Dordrecht., 2000.
4. Future Trends in Microelectronics. Up the Nano Creek / Ed. by S. Luryi., Xu J., A. Zaslavsky. – New York., 2007.
5. Nano and Molecular electronics: handbook / Ed. by S.E. Lyshevski. – Boca Raton, 2007.
6. Nanotechnology: an Introduction to Nanostructuring Techniques / Ed. by M. Kohler, W. Fritzsche. – New York., 2007.
7. Surface Modification and Mechanical Properties of Bulk Silicon. Tribology Issues and Opportunities in MEMS. / Ed. by Scherge, M.; Schaefer, J. – Kluwer Academic Publishers 1998.
8. Burrell, A.K. Synthetic routes to multiporphyrin. // Chem. Rev. – 2001. – Vol. 101. – P. 2751–2796.
9. Heymann, D.; Bachilo, S.; Weisman, B.; Cataldo, F. et al. $C_{60}O_3$ Fullerene Ozonide: Synthesis and Dissociation to $C_{60}O$ and O_2 . // J. Am. Chem. Soc. – 2000. – Vol. 122. – P. 11473–11479.
10. Heymann, D., Bachilo, S., Weisman, R., Ozonides, Epoxides, and Oxidooxanulenes of C_{70} . // J. Am. Chem. Soc. – 2002. – Vol. 124. – P.6317–6323.
11. Da Ros, T., Spallutto, G., Prato, M. Biological Applications of Fullerene Derivatives: A Brief Overview. Croatica Chemica Acta. – 2001. – Vol. 74(4). – P. 743–755.
12. Kodymová, J., Müllerová, A., Krása, J. et al. The Role of the Oxygen Molecule in the Photolysis of Fullerenes, Fullerene Sciences and Technology. – 2000. – Vol.8. – P. 289–318.
13. Mchedlov-Petrosyan, N., Klochov, V., Andrievsky, G. Colloidal dispersions of fullerene C_{60} in water: some properties and regularities of coagulation by electrolytes. // J. Chem. Soc., Faraday Trans. – 1997. – Vol. 93(24). – P.4343–4346.
14. Kaesarmann, F., Kempf, Ch. Buckminsterfullerene and Photodynamic Inactivation of Viruses. // Reviews in Medical Virology. – 1998. – Vol. 8. – P. 143–151.
15. Tagmatarchis, N. Carbon-based materials: From fullerene nanostructures to functionalized carbon nanotubes. // Pure Appl. Chem. – 2005. – Vol. 77. – P.675–1684.
16. Scharff, P.; Risch, K.; Carta-Abelmann et al. Structure of C_{60} fullerene in water: spectroscopic data. // Carbon. – 2004. – Vol. 42(5-6). – P. 1203–1206.
17. Song T., Dai S.; Tam K. Aggregation behavior of two-arm fullerene-containing poly (ethylene oxide). // Polymer. – 2003. – Vol. 44. – P.2529–2539.
18. Vilenko B., Sienkiewicz A., Lekka S. et al. In vitro assay of singlet oxygen generation in the presence of water-soluble derivatives of C_{60} . // Carbon. – 2004. – Vol. 42(5-6). – P. 1195–1198.
19. Webster R.D., Heath G.A., Voltammetric, EPR and UV-VIS-NIR spectroscopic studies associated with the one-electron oxidation of and in C_{60} C_{70} 1, 1', 2, 2'-tetrachloroethane containing tri-uroromethanesulfonic acid. // Phys. Chem. Chem. Phys. – 2001. – Vol. 3. – P. 2588–2594.
20. William B. D. Dependence of electron transfer dynamics in wire-like bridgemolecules on donor-bridge energetics and electronic interactions. // Chemical Physics. – 2002. – Vol. 281. – P. 333–346.
21. William B.D., Dependence of electron transfer dynamics in wire-like bridge molecules on donor-bridge energetics and electronic interactions. // Chemical Physics. – 2002. – Vol. 281. – P. 333–346.
22. Yoshida Y. Reactivity of $C_{60}C_{16}$ and $C_{60}Br_n$ ($n = 6, 8$) in Solution in the Absence and in the Presence of Electron Donor Molecules. // J. Am. Chem. Soc. – 2000. – Vol. 122. – P. 7244–7251.

Submitted on 31.01.13

О. Іванюта, канд. фіз.-мат. наук,
кафедра електрофізики, радіофізичний факультет
Київський національний університет імені Тараса Шевченка

ВЛАСТИВОСТІ ЗМІНЕНИХ ФУЛЕРИТІВ ДЛЯ ОРГАНІЧНИХ ФОТО ЧУТЛИВИХ ПРИСТРОЇВ

Змінені фулерити C_{mn} були виготовлені шляхом нерадіаційного опромінення і озонування C_{60} в гелієвому розчині. Експериментальні дослідження були проведені в ультрафіолетовому, видимому, інфрачервоному діапазоні спектрів раманієвської спектроскопією, XPS і АСМ. Структури змінених C_{mn} в гелієвому розчині (агрегати з гідратованими зв'язками) вивчалися. Я представляю результати від початкового вибору зразків, що ґрунтуються на інформації квантової структури і суттєвих властивостей, їх порівняння з результатами від обчислення щільності функціонала теорії для ефективності фотоелектричного пристрою на ефекті акцепторно – донорної архітектури. Порівняння спектральних особливостей змінених C_{mn} з даними для адсорбованих шарів дозволило виявити серії гідроксильних груп в змінених C_{mn} .

Ключові слова: фулерити C_{mn} , фулерол, гідроксил-, епоксил-, кето-зміни, електрона структура, збільшене поверхнєве інфрачервоне поглинання.

А. Иванюта, канд. физ.-мат. наук,
кафедра электрофизики, радиофизический факультет
Киевский национальный университет имени Тараса Шевченко

СВОЙСТВА ИЗМЕНЕННЫХ ФУЛЛЕРИТА ДЛЯ ОРГАНИЧЕСКИХ ФОТО ЧУВСТВИТЕЛЬНЫХ УСТРОЙСТВ

Измененные фуллерита C_{60} были изготовлены путем нерадиационного облучения и озонирования C_{60} в гелевом растворе. Экспериментальные исследования были проведены в ультрафиолетовом, видимом, инфракрасном диапазонах спектров рамановской спектроскопии, XPS и АСМ. Структуры измененных C_{60} в гелевом растворе (агрегаты с гидратированными связями) изучались. Я представляю результаты от первоначального выбора образцов, основываясь на информации о их квантовой структуре и сопутствующих свойствах, их сравнение с результатами вычисления плотности функционала в теории для эффективности фотоэлектрического устройства на эффекте акцепторных – донорной архитектуры. Сравнение спектральных особенностей измененных C_{60} данным для адсорбированных слоев позволило выявить серии гидроксильных групп в измененных C_{60} .

Ключевые слова: фуллериты C_{60} , фуллерол, гидроксиль-, эпоксил-, кето-изменения, электронная структура, увеличенное поверхностное инфракрасное поглощение.

UDC 004.(051+052+55)

A. Kotenko, post., D. Gryaznov, assist., Yu. Boyko, Ph.D.
Faculty of Radiophysics, Taras Shevchenko National University of Kyiv

OPTIMIZATION WEB-APPLICATIONS WITHOUT USERS GENERATED CONTENT FOR RELIABILITY AND PERFORMANCE USING NGINX TECHNOLOGY

The paper is considered to approach to develop reliable and productive web-application. Contradiction between performance, achieved by building system from different, dedicated to one task, nodes, and reliability is analyzed. Proposed technical solution based on nginx that eliminates the contradiction.

Keywords: web-applications, reliability, performance, nginx.

Introduction. Recently there has been continued growth in both the number of online users and Web applications (sites, services, social networks) [1]. The growing number of users requires a web application a significant increase in performance due to the fact that the process visits to web resources has a random nature with significant fluctuations. And customer service even visiting peaks should occur at the time of the order of 1–2 seconds [7]. At the same time the web application requires reliability, so even 15 minutes disability sites lead to a significant reduction of its position in Google SERP [6].

So actual is the problem of building Web applications that have improved reliability and performance simultaneously. But these IT requirements are often those that contradict each other. This contradiction occurs because that productivity is generally associated with parallel operation. This parallel operation requires some parts of specialization that prevents duplication of their work to ensure reliability.

Implementation. In this paper we propose a technical solution that is optimal in terms of reliability and performance. As the criteria of reliability, we used a disability, as well as performance criteria – the number of components that can perform the work at once.

To construct the solution we used technology nginx [4]. Nginx is a free, open-source, high-performance HTTP server and reverse proxy. Nginx was started in 2002, with the first public release in 2004. Nginx now hosts nearly 12.18% (22.2M) of active sites across all domains. Nginx is known for its high performance, stability, rich feature set, simple configuration, and low resource consumption. [5] Scheme of the standard Nginx configuration shown in Fig.1.

As can be seen from the scheme in the standard technology Nginx configuration ensures reliable operation in the case of a single server. However, any server can fail for a number of reasons such as hardware or software failure, network failure, or even problems with the electricity in the data center.

As can be seen from the scheme in the standard technology Nginx configuration ensures reliable operation in the case of a single server. However, any server can fail for a number of reasons such as hardware or software failure, network failure, or even problems with the electricity in the data center.

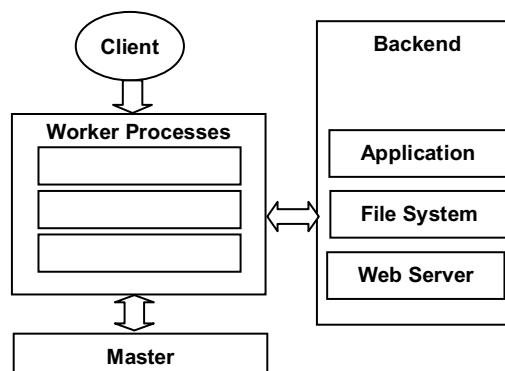


Fig. 1. Scheme of Nginx

The standard way to improve the reliability of system works is mirroring servers, and the reserve server can be located even in a different data center. In case of failure of one server it is possible to switch to another. However, the use of reserve systems can not improve the performance of the system as a whole, as the work performed by one anyway. To improve performance main and reserve servers have to serve clients simultaneously. It is clear, that in the case where users generate the content this architecture become complex because it requires synchronization of content between servers when the user change it. But there are a number of services, such as [3], where it is not necessary to modify the stored content in response to the user actions. The proposed solution is designed for these systems. The main idea of solution is to create mirrored copies of the service, access to which is performed under round robin, implemented by domain name system service [2]. Scheme of the round robin is shown in Fig. 2.

The main problem of this solution is that it requires storing complete copy of the data on all used servers and therefore takes up more memory than the parallel operation of specialized copies. As the solution of this problem it is proposed to use natural feature of database cache – keeping in memory the data that are used more commonly. But in order to work, data used to serve client's request has to hit the cache in the server. So, on every server users requests have to be limited to some subset, of